

Phytoplankton  
community structure  
in the North Sea

M. Thyssen et al.

# Phytoplankton community structure in the North Sea: coupling between remote sensing and automated in situ analysis at the single cell level

M. Thyssen<sup>1,\*</sup>, S. Alvain<sup>1</sup>, A. Lefèbre<sup>2</sup>, D. Dessailly<sup>1</sup>, M. Rijkeboer<sup>4</sup>, N. Guiselin<sup>1</sup>, V. Creach<sup>3</sup>, and L.-F. Artigas<sup>1</sup>

<sup>1</sup>Université Lille Nord de France – CNRS UMR 8187 Laboratoire d’Océanologie et de Géosciences, Université du Littoral Côte d’Opale, MREN, 32 Avenue Foch, 62930 Wimereux, France

<sup>2</sup>IFREMER LER, 150 quai Gambetta, 62200, Boulogne sur Mer, France

<sup>3</sup>The Centre for Environment, Fisheries and Aquaculture Science (Cefas), Pakefield Road, NR33 0HT Lowestoft, UK

<sup>4</sup>RWS Centre for Water Management, Laboratory for hydrobiological analysis, Zuiderwagenplein 2, 8224 AD Lelystad, the Netherlands

\* now at: Aix Marseille Université CNRS/INSU, IRD, Mediterranean Institute of Oceanography (MIO), UM 110, 13288 Marseille, France

Title Page

Abstract

Introduction

Conclusions

References

Tables

Figures



Back

Close

Full Screen / Esc

Printer-friendly Version

Interactive Discussion



Received: 1 October 2014 – Accepted: 6 October 2014 – Published: 7 November 2014

Correspondence to: M. Thyssen (melilotus.thyssen@mio.osupytheas.fr)

Published by Copernicus Publications on behalf of the European Geosciences Union.

**BGD**

11, 15621–15662, 2014

---

**Phytoplankton  
community structure  
in the North Sea**

M. Thyssen et al.

---

Title Page

Abstract

Introduction

Conclusions

References

Tables

Figures



Back

Close

Full Screen / Esc

Printer-friendly Version

Interactive Discussion



## Abstract

Phytoplankton observation in the ocean can be a challenge in oceanography. Accurate estimations of their biomass and dynamics will help to understand ocean ecosystems and refine global climate models. This requires relevant datasets of phytoplankton at a functional level and on a daily and sub meso scale. In order to achieve this, an automated, high frequency, dedicated scanning flow cytometer (SFC, Cytobuoy, NL), has been developed to cover the entire size range of phytoplankton cells whilst simultaneously taking pictures of the largest of them. This cytometer was directly connected to the water inlet of a pocket Ferry Box during a cruise in the North Sea, 8–12 May 2011 (DYMAPHY project, INTERREG IV A “2 Seas”), in order to identify the phytoplankton community structure of near surface waters (6 m) with a high resolution spacial basis ( $2.2 \pm 1.8$  km). Ten groups of cells, distinguished on the basis of their optical pulse shapes, were described (abundance, size estimate, red fluorescence per unit volume). Abundances varied depending on the hydrological status of the traversed waters, reflecting different stages of the North Sea blooming period. Comparisons between several techniques analyzing chlorophyll *a* and the scanning flow cytometer, using the integrated red fluorescence emitted by each counted cell, showed significant correlations. The community structure observed from the automated flow cytometry was compared with the PHYSAT reflectance anomalies over a daily scale. The number of matchups observed between the SFC automated high frequency in situ sampling and the remote sensing was found to be two to three times better than when using traditional water sampling strategies. Significant differences in the phytoplankton community structure within the two days for which matchups were available, suggest that it is possible to label PHYSAT anomalies not only with dominant groups, but at the level of the community structure.

### Phytoplankton community structure in the North Sea

M. Thyssen et al.

Title Page

Abstract

Introduction

Conclusions

References

Tables

Figures



Back

Close

Full Screen / Esc

Printer-friendly Version

Interactive Discussion



## 1 Introduction

Phytoplankton plays a major role in marine ecosystems as the most important primary producer in the ocean (Field et al., 1998). Phytoplankton is involved in the long-term trapping of atmospheric carbon and its role in carbon transfer from the upper ocean layers to deep waters highlight its influence on climate (Boyce et al., 2010; Marinov et al., 2010). Beyond its role in the carbon cycle, phytoplankton also plays a major role in modifying the biogeochemical properties of water masses by converting most of the inorganic matter into available organic matter (nitrogen, phosphate, silicate, sulfur, iron); and determining the structure of the trophic status of marine environments.

Given this importance, it is insufficient to use a single proxy, such as chlorophyll *a* measurements, for quantifying and qualifying phytoplankton over large scales when attempting to understand its role in biogeochemical processes (Colin et al., 2004). Such proxy does not reflect changes in community structure (Hirata et al., 2011) and do not yield robust biomass estimations (Kruskopf and Flynn, 2006). Yet this classical proxy is frequently used to study the spatial and temporal variability of phytoplankton from both remotely sensed and in situ measurements. Le Quéré (Le Quéré et al., 2005) pointed out the importance of taking into account the functionality of phytoplankton species when considering the influence of phytoplankton community structure on biogeochemical processes. This functionality concept (i.e. Phytoplankton Functional Types, PFT) is described as set of species sharing similar properties or responses in relation to the main biogeochemical processes such as the N, P, Si, C and S cycles (diazotrophs for N cycle such as Cyanobacteria, DMSP producers for P cycle such as *Phaeocystis*, silicifiers for Si cycle such as Diatoms, calcifiers for C cycle such as Coccolithophorids, size classes, motility, food web structure mainly used for C cycle).

Representative data sets of phytoplankton functional types, size classes and specific chlorophyll *a* concentrations are the subject of active research using high frequency in situ dedicated analysis from automated devices such as spectral fluorometers, particle scattering and absorption spectra recording instruments, or automated and

BGD

11, 15621–15662, 2014

### Phytoplankton community structure in the North Sea

M. Thyssen et al.

Title Page

Abstract

Introduction

Conclusions

References

Tables

Figures



Back

Close

Full Screen / Esc

Printer-friendly Version

Interactive Discussion



---

## Phytoplankton community structure in the North Sea

M. Thyssen et al.

---

[Title Page](#)[Abstract](#)[Introduction](#)[Conclusions](#)[References](#)[Tables](#)[Figures](#)[Back](#)[Close](#)[Full Screen / Esc](#)[Printer-friendly Version](#)[Interactive Discussion](#)

remotely controlled scanning flow cytometry (SFC). Among the high frequency in situ techniques used to quantify phytoplankton abundance, community structure and dynamics, SFC is the most advanced instrument, counting and recording cell optical properties at the single cell level. This technology has recently been adapted for the analysis of almost all the phytoplankton size classes and focuses on the resolution of phytoplankton community structure dynamics (Dubelaar et al., 1999; Olson et al., 2003; Sosik et al., 2003; Thyssen et al., 2008a, b). In parallel, remote sensed algorithms have been developed which are dedicated to characterizing phytoplankton groups, PFTs or size classes (Sathyendranath et al., 2004; Ciotti et al., 2006; Nair et al., 2008; Aiken et al., 2008; Kostadinov et al., 2010; Uitz et al., 2010; Moisan et al., 2012). One of these algorithms, PHYSAT, has provided a description of the dominant phytoplankton functional types (Le Quéré et al., 2005) for open waters on a global scale, leading to various studies concerning the PFT variability (Alvain et al., 2005, 2013; Masotti et al., 2011; Demarcq et al., 2011). PHYSAT relies on the identification of water-leaving radiance spectra anomalies, empirically associated with the presence of specific phytoplankton groups in the surface water. The anomalies were labeled thanks to the comparison with high pressure liquid chromatography biomarker pigment match ups. To date, six dominant phytoplankton functional groups in open waters (Diatoms, Nanoeukaryotes, *Prochlorococcus*, *Synechococcus*, *Phaeocystis*-like, Coccolithophorids) have been found to be significantly related to specific water-leaving radiance anomalies from SeaWiFS (Sea-viewing Wide Field-of-view Sensor) sensor measurements at a resolution of 9 km (Alvain et al., 2008). These relationships have been verified by theoretical optical models (Alvain et al., 2012). This theoretical study also showed that additional groups or assemblages could be added in the future, once accurate in situ observations are available. Describing the community structure on a regional scale will give better quantification and understanding of the phytoplankton responses to environmental change and consequently, support the modification of theoretical considerations regarding energy fluxes across trophic levels. It is critical in understanding community structure interactions and particularly when it

---

## Phytoplankton community structure in the North Sea

M. Thyssen et al.

---

[Title Page](#)[Abstract](#)[Introduction](#)[Conclusions](#)[References](#)[Tables](#)[Figures](#)[Back](#)[Close](#)[Full Screen / Esc](#)[Printer-friendly Version](#)[Interactive Discussion](#)

is necessary to take into account the meso-scale structure in a specific area (D'Ovidio et al., 2010), which is the case in areas under the influence of regional physical forcing such as the English Channel and the North Sea. Long-term changes detected in these regions have been shown to impact local ecosystem functioning by inducing, for instance, a shift in the timing of the spring bloom (Wiltshire and Manly, 2004; Sharples et al., 2009; Vargas et al., 2009; Racault et al., 2013) or specific migrations of regional (Gomez and Souissi, 2007) or dominant phytoplankton groups (Widdicombe et al., 2010). In addition, hydrodynamic conditions have been shown to play a strong role in the phytoplankton distribution on a regional scale (Gailhard et al., 2002; Leterme et al., 2008). It is therefore crucial to develop specific approaches to characterize the phytoplankton community structure (beyond global-scale dominance) and its high frequency variation in time and space. In order to achieve this, large data sets of in situ analyses resolving PFT are essential for specific calibration and validation of regional remote sensing algorithms such as PHYSAT. Flow-through surface water properties analysis for remote sensing calibration optimizes the amount of matchups (Werdell et al., 2010; Chase et al., 2013). For the purpose of collecting high resolution in situ phytoplankton community structure, automated SFC technology allows samples to be collected at high frequency, resolving hourly and km scales in a totally automated system. The instrument enables single cell analysis of phytoplankton from 1 to 800  $\mu\text{m}$  and several mm in length for chain forming cells and automated sampling allows large space and time domains to be covered at a high resolution (Sosik et al., 2003; Thyssen et al., 2008b, 2009; Ribalet et al., 2010).

Based on this approach, a high frequency study of the phytoplankton community structure in the North Sea was conducted. The in situ observations have been used to label PHYSAT anomalies, showing the potential of such in situ and remote sensed data coupling. Thus, the available dataset makes it possible to distinguish between different water-leaving radiance anomaly signatures in which significant distinct phytoplankton community structures can be described, rather than just the dominant communities, as it is the case of previous studies. Our results are an improvement over conventional

approaches as they allow the distribution of phytoplankton community structure to be characterized at a high resolution, from both in situ and day-to-day water-leaving radiance anomaly maps specific to the study area.

## 2 Materials and methods

5 Samples were collected during the PROTOOL/DYMAPHY-project cruise onboard the RV *Cefas Endeavour* from the 8 to 12 May 2011 in the south-west region of the North Sea (Fig. 1). Automated coupled sampling using a Pocket FerryBox (PFB) and a Cytosense scanning flow cytometer (SFC, CytoBuoy, b.v.) started on the 8 May at 09:00 UTC and ended on the 12 May at 04:00 UTC. Water was continuously collected  
10 from a depth of 6 m and entered the PFB at a pressure of 1 bar maximum. Sub-surface discrete samples were collected using Niskin bottles on a rosette and analyzed using a second Cytosense SFC (Stations 4, 6 and 13 were used in this paper, Fig. 1).

### 2.1 Phytoplankton community structure from automated SFC

15 Phytoplankton abundance and group description were determined by using two Cytosense SFCs (CytoBuoy, b.v.). These instruments are dedicated to phytoplankton single cell recording, enabling cells from 1 to 800  $\mu\text{m}$  and several mm in length to be analysed routinely in 1–10  $\text{cm}^3$ . For the automated measurements, samples for SFC were automatically collected from a 450  $\text{cm}^3$  sampling unit where water from the continuous flow was periodically stabilized. This sampling unit was designed to  
20 collect bypass water from the 1 bar PFB inlet. The sampling unit water was replaced within a minute. One of the Cytosenses was directly connected to the sampling unit and two successive analyses with two distinct protocols were scheduled automatically every 10 min. A calibrated peristaltic pump was used to estimate the analysed volumes. Suspended particles were then separated using a laminar flow and subsequently  
25 crossed a laser beam (Coherent, 488 nm, 20 mV). The instrument recorded the

BGD

11, 15621–15662, 2014

## Phytoplankton community structure in the North Sea

M. Thyssen et al.

Title Page

Abstract

Introduction

Conclusions

References

Tables

Figures



Back

Close

Full Screen / Esc

Printer-friendly Version

Interactive Discussion





by using the low sensitivity PMTs that behaved linearly below this value with the high sensitivity PMT.

Discrete samples were collected during the cruise and analyzed using a second Cytosense SFC equipped with the Image in Flow system. The samples were analysed using settings similar to those of the Cytosense coupled to the PFB and pictures were randomly collected for the largest particles until the predetermined number of pictures was reached.

## 2.2 Temperature and salinity

The PFB (4H-JENA©) was fixed on the wet laboratory bench, close to the Cytosense, in order to share the same water inlet. This instrument recorded temperature and conductivity (from which salinity was computed) from the clean water supplied by the ships seawater pumping system at a frequency of one sample every minute.

Within the PFB dataset, only data related to automated SFC analyses were selected for plotting temperature–salinity diagrams.

## 2.3 Chlorophyll *a*

Samples for High Pressure Liquid Chromatography (HPLC) analyses and bench top fluorometry (Turner® fluorometer) were collected randomly within 6 h periods before or after the supposed MODIS (Moderate Resolution Imaging Spectroradiometer) sensor passage (12:30 p.m. UTC) to fulfill classical requirements in terms of in situ and remotely sensed matchup criteria. Samples were collected from the outlet of the PFB, filtered onto GF/F filters and stored directly in a –80 °C freezer. The HPLC analyses were run on an Agilent Technologie, 1200 series. Pigments were extracted using 3 cm<sup>3</sup> ethanol containing vitamin E acetate as described by Claustre et al. (2004) and adapted by Van Heukelem and Thomas (2001). For bench top fluorometry, the filters were subsequently extracted in 90 % acetone. Chlorophyll *a* (chl *a*) concentration was evaluated by fluorometry using a Turner Designs Model 10-AU fluorometer. The

### Phytoplankton community structure in the North Sea

M. Thyssen et al.

Title Page

Abstract

Introduction

Conclusions

References

Tables

Figures



Back

Close

Full Screen / Esc

Printer-friendly Version

Interactive Discussion



fluorescence was measured before and after acidification with HCl (Lorenzen, 1966). The fluorometer was calibrated using known concentrations of commercially purified chl *a* (Sigma-Aldrich®).

The PFB was equipped with a multiple fixed wavelength spectral fluorometer (AOA fluorometer, bbe©) sampling once every minute to obtain chl *a* values.

MODIS chl *a* values were extracted from daily level 2 product determining with a 4 km resolution (L3 Binned data).

## 2.4 Mixed layer depth

Daily water column temperature mapping was obtained from the Forecasting Ocean Assimilation Model 7 km Atlantic Margin model (FOAM AMM7), available at MyOcean data base (<http://www.myocean.eu.org/>). Model output temperature depths were as follows: 0, 3, 10, 15, 20, 30, 50, 75, 100, 125, 150 m. Average mixed layer depth (MLD) on the 5 sampling days was calculated from daily temperature datasets. MLD was defined as the absolute temperature difference of more than 0.2 °C from one depth to the surface (defined at 10 m, de Boyer Montégut et al., 2004).

## 2.5 Matching method between in situ and remote sensed observations for phytoplankton community structure

Remotely sensed observations were selected on the basis of quality criteria that ensured a high degree of confidence in PHYSAT as described in Alvain et al. (2005). Thus, pixels were only considered when clear sky conditions were found and when the optical thickness, a proxy of the atmospheric correction steps quality, was lower than 0.15. In addition, as the region of interest included some coastal areas, that are not considered as open waters for remote sensing, we have selected pixels according to their optical properties (Vantrepotte et al., 2012). Consequently, this avoided using waters rich in sediment which previously rendered it impossible to use the PHYSAT version. Waters classified as turbid were therefore excluded from

BGD

11, 15621–15662, 2014

### Phytoplankton community structure in the North Sea

M. Thyssen et al.

Title Page

Abstract

Introduction

Conclusions

References

Tables

Figures

◀

▶

◀

▶

Back

Close

Full Screen / Esc

Printer-friendly Version

Interactive Discussion



the empirical relationship since the PHYSAT method is currently not available for such areas. Waters classified as non-turbid using the same criteria were selected and the PHYSAT algorithm applied. To link coincident in situ and remotely sensed observations, a match-up exercise was carried out. Matching points between in situ SFC samples (considered as in situ data) and 4 km resolution MODIS pixels were selected by comparing their concomitant position day after day. When more than one in situ SFC sample was found in a MODIS pixel the averaged value of TFLR (a.u. cm<sup>-3</sup>) for each phytoplankton group was calculated. From the matching points, the PHYSAT method resulted in water leaving irradiance anomalies spectra (Ra) as described in Alvain et al. (2008, 2012).

## 2.6 Statistics

Statistics were run under R software (CRAN, <http://cran.r-project.org/>). Before running correlation and comparison tests on the different in situ sensors (for chl *a* and Total TFLR), the Shapiro normality test was run. When Normality was not applied, a Wilcoxon signed rank test was applied. Correlations between data were defined using Spearman's rank correlation coefficient.

As the PHYSAT approach is based on the link between specific Ra spectra (in terms of shapes and amplitudes) and specific phytoplankton composition, the set of remote sensed data was separated into distinct groups with similar Ra. The PHYSAT Ra found over the studied area and matching the in situ SFC samples was differentiated by applying a *k*-means clustering partitioning method (tested either around means (Everitt and Hothorn, 2006) or around centroids (Kaufman and Rousseeuw, 1990)). The appropriate number of clusters was decided with a plot of the within groups sum of squares by number of clusters extracted. A hierarchical clustering was computed to illustrate the *k*-means clustering method. Within each *k*-mean cluster, SFC-defined phytoplankton community was described and differences between TFLR cm<sup>-3</sup> per phytoplankton group were compared within the different PHYSAT spectra clusters using the Wilcoxon signed rank test.

## Phytoplankton community structure in the North Sea

M. Thyssen et al.

Title Page

Abstract

Introduction

Conclusions

References

Tables

Figures



Back

Close

Full Screen / Esc

Printer-friendly Version

Interactive Discussion



### 3 Results

#### 3.1 Temperature, salinity and mixed layer depth

The sampling track crossed three North Sea marine zones: Western Humber, Tyne, Dogger, Eastern Humber and Thames (Fig. 1). The PFB measured temperature associated to the SFC samples and varied between 8.83 and 12.39 °C with an average of  $10.67 \pm 0.72$  °C. Minimal temperatures were found in the western Humber area (53–55° N and –1 to 1° E) and maximal temperatures were found in the Thames area (54–52° N, 2–4° E) (Fig. 2a). Salinity from the PFB ranged between 34.02 and 35.07 with an average value of  $34.6 \pm 0.26$ . Highest salinity values were found in the Dogger area above 55° N and in the limit between the Humber and the Thames areas, 53° N. Lowest salinity values were found in the Tyne area around 55° N, –1° E and in the Thames area (by the Thames plume; Fig. 2b).

The mixed layer depth calculated from the FOAM AMM7 was used to illustrate the physical environment of the traversed water masses. Different mixed layer depth characterized the sampled area, with deeper MLD in the northern part (15 to 30 m) and a shallower MLD in the southern area (~ 10 m, Fig. 1). A tongue of shallow MLD (~ 10 m) surrounded by deeper MLD (~ 20 m) crossed the sampling area at ~ 55° N and ~ 3° W.

#### 3.2 Phytoplankton community from SFC analysis

A total of 247 SFC validated analysed samples were collected during this experiment. Average distance between samples collected with the automated SFC was of  $2.2 \pm 1.8$  km when the system ran continuously. The sampling rate was  $25 \pm 45$  min. Up to 10 phytoplankton clusters were resolved (Fig. 3) based on their optical fingerprints from SFC analysis. The 10 discriminated clusters were labeled as follows: PicoORG cluster (Fig. 3a), PicoRED cluster (Fig. 3a), NanoSWS cluster (Fig. 3b), NanoRED1 cluster (Fig. 3c), NanoRED2 cluster (Fig. 3b and c); Micro1 cluster (Fig. 3c and d),

BGD

11, 15621–15662, 2014

### Phytoplankton community structure in the North Sea

M. Thyssen et al.

Title Page

Abstract

Introduction

Conclusions

References

Tables

Figures



Back

Close

Full Screen / Esc

Printer-friendly Version

Interactive Discussion



MicroLowORG (Fig. 3a), NanoORG and MicroORG clusters (Fig. 3d) and a cluster of large cells, Micro2 cluster (Fig. 3d). Pictures were randomly collected (between 20 and 60 pictures per sample within the Micro2 cluster) and were used to illustrate the most frequently encountered class (Fig. 4). Station 4 (Fig. 4a) sampled at 12 m, showed mostly a mixture of dinoflagellate-like cells (25 pictures collected within 47 counted cells). Station 6 (Fig. 4b) sampled at 7 m, showed pictures composed mainly of diatoms (*Thalassiosira* and *Chaetoceros*, 11 images collected among 28 counted cells). Station 13 (Fig. 4c) sampled at 7 m, gave a mixture of diatoms and dinoflagellates (58 pictures shot among the 99 counted cells corresponding to the Micro2 cluster: 5 *Chaetoceros*, 30 *Rhizosolenia*, 10 Dinoflagellates, one flagellate and several unidentified cells).

Cell abundance, average cell size and TFLR $\text{cm}^{-3}$  for each cluster are illustrated on Figs. 5–7 respectively. Average abundance and sizes of each cluster are addressed in Table 1. PicoRED cells were on average, the most abundant in the studied area (Fig. 5b and Table 1) followed by NanoRED2, PicoORG, NanoRED1 and Micro1 (Fig. 5f, a, c and g respectively, Table 1). The other cluster's abundances were below  $1 \times 10^2 \text{ cells cm}^{-3}$  on average (Fig. 5d, e, h, i, and j; Table 1). PicoORG cells were the smallest estimated (Fig. 6a, Table 1), while the largest estimated were MicroORG, MicroLowORG and Micro2 cells (Fig. 6h–j respectively, Table 1).

The western Humber zone (Fig. 1) was marked by the highest abundances of PicoRED, PicoORG, MicroORG, MicroLowORG and Micro1 (Fig. 5b, a, h, i and g). The eastern part of the Humber zone (Fig. 1) was marked by the highest abundances of NanoRED1 and Micro1 (as for the western part) (Fig. 5c and g). High values of PicoRED were also observed in this part of the Humber zone. The Tyne zone (Fig. 1) had the highest abundance of NanoORG and Micro2 clusters (Fig. 5d and j), and the lowest abundance of PicoRED and NanoSWS. High abundance values of MicroORG were also observed (Fig. 5h). The size of the NanoSWS and the NanoRED2 were the greatest in this zone (Fig. 6e and f). The Dogger zone (Fig. 1) was dominated in terms of abundance by the PicoRED and the PicoORG, where the sizes were the smallest (Fig. 6b and a) but did not show the highest abundance values. The cell sizes

BGD

11, 15621–15662, 2014

## Phytoplankton community structure in the North Sea

M. Thyssen et al.

Title Page

Abstract

Introduction

Conclusions

References

Tables

Figures



Back

Close

Full Screen / Esc

Printer-friendly Version

Interactive Discussion



of Micro1 were the greatest in this zone (Fig. 6g). Observations in the Thames zone (Fig. 1) produced the maximal abundance of NanoSWS and NanoRED2 (Fig. 6e and f). Sizes were the greatest for PicoORG, NanoRED1 and NanoSWS (together with the Tyne zone; Fig. 6a, c and e). TFLR follows similar trends to abundance (Fig. 7).

### 3.3 Comparison between scanning flow cytometry, Total Red Fluorescence and chlorophyll *a* analysis

Several bench top and in situ instruments, i.e. HPLC, Turner fluorometer and the PFB AOA fluorometer, were used to give either exact and/or proxy values of chl *a*. Similarly to temperature and salinity, the PFB AOA fluorometer samples were selected to match SFC samples. Overall values of chl *a* originating from these instruments were superimposed to the Total TFLR  $\text{cm}^{-3}$  (by summing up the TFLR  $\text{cm}^{-3}$  values of the observed cluster) and the MODIS chl *a* values matching the points on Fig. 8. HPLC values varied between 0.21 and 7.58  $\mu\text{g dm}^{-3}$  with an average of  $1.57 \pm 2.01 \mu\text{g dm}^{-3}$ . Turner fluorometer values varied between 0.41 and 2.31 with an average of  $1.24 \pm 0.7 \mu\text{g dm}^{-3}$ . AOA fluorometer values varied between 0.73 and 28.53  $\mu\text{g dm}^{-3}$  with an average of  $4.44 \pm 5.54 \mu\text{g dm}^{-3}$ . The Total TFLR  $\text{cm}^{-3}$  from SFC, normalized with 3  $\mu\text{m}$  bead red fluorescence varied between 5011 and 399 200 a.u.  $\text{cm}^{-3}$  with an average value of  $64\,394.5 \pm 67\,488.4 \text{ a.u. cm}^{-3}$ . The Shapiro normality test showed non normality for each of the variables so a Wilcox test was run between techniques involving similar units. HPLC and Turner chl *a* concentrations were significantly not different ( $n = 9$ ,  $p = 0.65$ ) and the correlation was significant (Spearman,  $r = 0.98$ , Table 2). The absolute values from both techniques were significantly different from the AOA fluorometer values ( $n = 9$ ,  $p < 0.001$  for both) but were significantly correlated (Spearman,  $r = 0.86$  and  $r = 0.82$  for HPLC and Turner fluorometer respectively, Table 2). The SFC Total TFLR (a.u.  $\text{cm}^{-3}$ ) summing up the TFLR of all the phytoplankton groups was used for comparison with other chl *a* determinations. Correlations with the AOA fluorometer, the HPLC and the Turner fluorometer results were all significant as shown in Table 2.

Title Page

Abstract

Introduction

Conclusions

References

Tables

Figures



Back

Close

Full Screen / Esc

Printer-friendly Version

Interactive Discussion



### 3.4 PHYSAT anomalies and SFC phytoplankton community composition, extrapolation to the non-turbid classified waters in the North Sea

Considering our database of coincident SFC in situ and MODIS remote sensed observations, a total of 56 matching points were identified, from which only 38 points corresponded to non-turbid classified waters. Matching points between in situ sampling and remote sensing pixels for the purpose of the PHYSAT empirical calibration were selected in the daytime period 06:00–18:00 UTC, the limit of the correlation significance between MODIS chl *a* and the AOA fluorometer chl *a* within the SFC dataset ( $r = 0.49$ ,  $\rho = 0.06$ ,  $n = 15$ , Spearman rank test), leaving 15 SFC matching points (Figs. 1 and 8). The chl *a* values found in the matching points were lower than  $0.5 \mu\text{g dm}^{-3}$  (Fig. 8).

PHYSAT radiance anomalies (Ra) were separated into two distinct anomalies using the within sum of square minimization (Fig. 9a) and illustrated on a dendrogram (Fig. 9b). These two distinct types of anomalies in terms of shape and amplitude are illustrated in Fig. 9c and d and the anomaly characteristics are summarized on Table 3. The first anomaly set (N1, Table 3) was composed of 5 spectra that had overall higher values than the second anomaly set (N2, Table 3), composed of the other 10 spectra. The corresponding SFC cluster proportion of  $\text{TFLR cm}^{-3}$  to the overall Total  $\text{TFLR cm}^{-3}$  found within the two anomalies are illustrated in Fig. 10a and b. Similarly, the relative difference of each phytoplankton cluster's  $\text{TFLR cm}^{-3}$  within the two anomalies to its overall  $\text{TFLR cm}^{-3}$  median value are illustrated in Fig. 10c and d. Considering our previous analyses, N1 and N2 community structures were dominated by NanoRED2  $\text{TFLR cm}^{-3}$  (Fig. 10a and b). Regarding each distinct cluster relative difference to its overall median value, samples corresponding to N1 anomalies had significantly higher NanoRED1  $\text{TFLR cm}^{-3}$ , higher NanoORG  $\text{TFLR cm}^{-3}$  and higher MicroORG  $\text{TFLR cm}^{-3}$ ; while the samples corresponding to N2 anomalies had only higher PicoRED  $\text{TFLR cm}^{-3}$  (Wilcoxon rank test, N1,  $n = 5$ ; N2,  $n = 10$ , Fig. 10c and d). Temperature, salinity, MODIS chl *a* and SFC Total  $\text{TFLR cm}^{-3}$  found in each in situ sample corresponding to both sets of anomalies are illustrated in Fig. 11. Samples

BGD

11, 15621–15662, 2014

## Phytoplankton community structure in the North Sea

M. Thyssen et al.

Title Page

Abstract

Introduction

Conclusions

References

Tables

Figures



Back

Close

Full Screen / Esc

Printer-friendly Version

Interactive Discussion



found in the N1 pixels were significantly warmer ( $11.3 \pm 0.32$  °C in N1 and  $10.94 \pm 0.23$  °C in N2,  $p < 0.1$ , Wilcoxon rank test, Fig. 11a), not significantly different in terms of salinity, although N1 waters were less salty (Fig. 11b), significantly richer in chl *a* ( $p < 0.01$ , Wilcoxon rank test, Fig. 11c), but not significantly different in Total TFLR  $\text{cm}^{-3}$  values (Fig. 11d).

Considering the specificity of each set of Ra in terms of phytoplankton and environmental conditions, it's interesting to map their frequency of detection in our area of interest. A pixel is associated to an anomaly when the Ra values at each wavelength fulfilled the criteria of Table 3. The frequencies of occurrence over the sampling period based on a synthesis overlapping the sampling period are illustrated in Fig. 12a and b. Pixels corresponding to N1 anomaly were mostly found in the 54–56° N area (Dogger and German, Fig. 1), following the edge between the shallow MLD tong and the deepest MLD zones (Fig. 1), but also near the Northern Scottish coast (Forth, Forties and Cromarty, Fig. 12a), where MLD was shallow (Fig. 1). The N2 anomaly pixels were mostly found in the Forties, Fisher and German area, on much smaller surfaces (Fig. 12b).

## 4 Discussion

The automated SFC used during this study resolves the spacial/temporal issue by its high frequency sampling, reaching sub mesoscale distribution and diel changes in abundances. However, water mass dynamics generates micro patchiness which modifies phytoplankton community structure and makes it difficult to follow a population over time and at a basin scale. In this context, the daily extrapolation of the community structure using PFT daily remote sensing mapping can help to follow spatial distribution of phytoplankton communities. The improvement of PFT mapping, i.e. from dominant groups to the community structure resolution, is one of the ideas generated in this paper. This is a first attempt to combine plankton community structure using automated flow cytometry and PHYSAT over a daily scale. Of course, there needs to be many

## BGD

11, 15621–15662, 2014

### Phytoplankton community structure in the North Sea

M. Thyssen et al.

Title Page

Abstract

Introduction

Conclusions

References

Tables

Figures



Back

Close

Full Screen / Esc

Printer-friendly Version

Interactive Discussion



more matchups at this scale in order to identify precisely the PHYSAT anomalies with a community structure. A recent publication that enables the classification of a large range of anomaly spectra (Ben Mustapha et al., 2014) should help to make this easier. Thus, the knowledge and the tools are available, which augurs well for understanding phytoplankton heterogeneity and variability over high frequency spatio-temporal scales.

Indeed, resolving phytoplankton community structure over the sub meso scale and hourly scale is a good way to understand the influence of environmental short scale events (Thyssen et al., 2008a; Lomas et al., 2009), seasonal (or not) succession schemes, resilience capacities of the community after environmental changes and impacts on the specific growth rates (Sosik et al., 2003). Resolving the community structure and the causes of variations at several temporal and spatial scales has great importance in further understanding the phytoplankton functional role in biogeochemical processes. This scale information is currently lacking for the global integration of phytoplankton in biogeochemical models, mainly due to the lack of adequate technology which are needed to integrate the different levels of complexity linked to phytoplankton community structure.

Phytoplankton community structure from automated SFC is described through clusters of analyzed particles sharing similar optical properties. Most of the clusters could be described at the plankton functional type level (Le Quéré et al., 2005), because of some singular similarities combining geographical area, abundance, size, pigments and structure proxies obtained from optical SFC variables (Chisholm et al., 1988; Veldhuis and Kraay, 2000; Rutten et al., 2005; Zubkov and Burkill, 2006). The Cytobuoy instrument used in this study was developed to identify phytoplankton cells from picophytoplankton up to large microphytoplankton with complex shapes, even those forming chains. Indeed, the volume analyzed was close to  $3\text{ cm}^3$ , giving accurate counts of clusters with abundances as low as  $30\text{ cells cm}^{-3}$  (100 cells counted), under which, coefficient of variation exceeds 10% (Thyssen et al., 2008a). Such low abundances were found for some of the clusters identified in this study (NanoORG, MicroORG and Micro2 clusters for which the median abundance value was

## BGD

11, 15621–15662, 2014

### Phytoplankton community structure in the North Sea

M. Thyssen et al.

[Title Page](#)

[Abstract](#)

[Introduction](#)

[Conclusions](#)

[References](#)

[Tables](#)

[Figures](#)



[Back](#)

[Close](#)

[Full Screen / Esc](#)

[Printer-friendly Version](#)

[Interactive Discussion](#)





et al., 2002). The observed abundances did fit with the low *Coccolithophoridae* concentrations observed in the southern North Sea (Houghton, 1991).

The Micro2 cluster was mostly composed of large diatoms (*Rhizosolenia*, *Chaetoceros*) and dinoflagellates (Fig. 4) within the size range of 40–100  $\mu\text{m}$  (Fig. 6j) as observed in the pictures (Fig. 4). The presence of these groups illustrates the boundary between the end of the diatom bloom and the development of a dinoflagellate bloom, from which it could be possible to make a link with the *Dinophysis norvegica* and *Alexandrium* early summer bloom, observed in the Tyne region by Dodge et al., 1977 (Dodge, 1977). This is in agreement with the stratification observed within the Thames zone (Fig. 1).

The data sets from the spacial (km) and the temporal (hourly) scales for phytoplankton community structure based on single cell optical properties are important for validating the methods for describing phytoplankton community structure from space. Ocean algorithms need specific information on water properties and phytoplankton structure and are dependent on validation from in situ observations, always complex to collect and limited by sky condition criteria. The PHYSAT method was built on in situ HPLC analysis and the most reliable relationship between them was found in an empirical relationship based on dominant phytoplankton functional types, missing the possible contribution of less dominant, but still important, phytoplankton functional types defining the community structure. The remote sensing synoptical extrapolation concerning phytoplankton community structure remains to be established and in spite of a theoretical validation (Alvain et al., 2012), still depends on important in situ data point collection in order to build robust empirical relationships. In this study, the combination of phytoplankton high frequency analysis from an automated SFC with the PHYSAT method proved to be an excellent calibration by giving an unprecedented amount of matching points for only two significant sampling days (number of analyzed samples for non-turbid waters matching MODIS pixels: 38, number of used samples between 06:00 and 18:00 UTC: 15, corresponding to 39.5 % profitability), compared to the 14 % matching points from the GeP&CO dataset (Alvain et al., 2005).

Phytoplankton  
community structure  
in the North Sea

M. Thyssen et al.

Title Page

Abstract

Introduction

Conclusions

References

Tables

Figures



Back

Close

Full Screen / Esc

Printer-friendly Version

Interactive Discussion



---

## Phytoplankton community structure in the North Sea

M. Thyssen et al.

---

[Title Page](#)[Abstract](#)[Introduction](#)[Conclusions](#)[References](#)[Tables](#)[Figures](#)[Back](#)[Close](#)[Full Screen / Esc](#)[Printer-friendly Version](#)[Interactive Discussion](#)

The coupling of SFC and PHYSAT has shown that a first set of specific anomalies (N1) can be associated to NanoRED1, NanoORG and MicroORG, which contributed more to the Total TFLR $\text{cm}^{-3}$  (a proxy of chl *a*, Fig. 7, Table 2) than in the second set of anomaly (N2), in which PicoRED cells contributed significantly more to the Total TFLR $\text{cm}^{-3}$ , but also, where Micro1 contribution to Total TFLR $\text{cm}^{-3}$  was above its overall median value observed along the matching points (Fig. 10d). Spatial successions between diatoms and cryptophytes revealed differences in stratification, lower salinity and shallower MLD (Moline et al., 2004; Mendes et al., 2013). Indeed, the N1 anomaly corresponds to areas of low MLD (Fig. 1) following the main North Sea current from the south west to the north east (Holligan et al., 1989), surrounding the Dogger bank. This anomaly was also found on the north-western part of the northern North Sea, following the Scottish coastal water current with a shallow MLD (Figs. 1 and 11a). The N2 anomaly was observed with the deeper MLD of the Forties, Fisher and German areas (Figs. 1 and 11b). These N2 areas corresponded to a phytoplankton community still blooming while the N1 anomaly areas might be at a stage of late blooming, in which conditions fit cryptophyceae development and grazing (cells of *Myrionecta rubra* were observed when using the Image in Flow, not shown). These organisms were found dominating the areas surrounding the Dogger bank from observations and counts carried out by Nielsen et al. (1993) during the same period.

Previous comparisons between bench top flow cytometry and remote sensing (Zubkov and Quartly, 2003) could technically not include the entire size range of nano-microphytoplankton. The Cytobuoy SFC resolves cells up to 800  $\mu\text{m}$  in theory, but this depends on the counted cells in the volume sampled (reaching 3  $\text{cm}^3$ , which is approximately ten times more than classical flow cytometry). However, the largest part of phytoplankton production in the North Sea is driven by cells < 20  $\mu\text{m}$  (Nielsen et al., 1993), and we can consider this size class to be correctly counted with the SFC.

In conclusion, the use of automated SFC Cytosense technology is an area of great interest when coupled with remote sensing algorithms in the study of surface

phytoplankton distribution. Further advances in understanding the link between the phytoplankton community composition and distribution, with radiance anomalies are expected from improvements in analyzing larger volumes by automated SFC and by substantially increasing the number of coincidences between remote sensing and in situ observations.

*Acknowledgements.* This study was funded by the DYMPAHY (Development of a DYnamic observation system for the assessment of MARine water quality, based on PHYtoplankton analysis) INTERREG IVA “2 Mers Seas Zeeën” European cross-border project, co-funded by the European Regional Development Fund (ERDF) and French (ULCO-CNRS-UL1), English (Cefas) and Dutch (RWS) partners. We thank the captain and crew of the RV *Cefas Endeavour*, as well as Anne-Hélène Rêve for chlorophyll *a* bench top analysis. We also thank Rodney Forster for his invitation onboard the ship during the EU FP7 PROTOOL (Automated Tools to Measure Primary Productivity in European Seas) cruise. We are also grateful to our funding sources, the CNRS, the CNES-TOSCA/PHYTOCOT project. The authors thank NASA/GSFC/DAAC for providing access to daily L3 MODIS binned products.

## References

- Aiken, J., Hardman-Mountford, N. J., Barlow, R., Fishwick, J., Hirata, T., and Smyth, T.: Functional links between bioenergetics and bio-optical traits of phytoplankton taxonomic groups: an overarching hypothesis with applications for ocean colour remote sensing, *J. Plankton Res.*, 30, 165–181, 2008.
- Alvain, S., Moulin, C., Dandonneau, Y., and Bréon, F. M.: Remote sensing of phytoplankton groups in case 1 waters from global SeaWiFS imagery, *Deep-Sea Res. Pt. I*, 52, 1989–2004, 2005.
- Alvain, S., Moulin, C., Dandonneau, Y., and Loisel, H.: Seasonal distribution and succession of dominant phytoplankton groups in the global ocean: a satellite view, *Global Biogeochem. Cy.*, 22, GB3001, doi:10.1029/2007GB003154, 2008.
- Alvain, S., Loisel, H., and Dessailly, D.: Theoretical analysis of ocean color radiances anomalies and implications for phytoplankton groups detection in case 1 waters, *Opt. Express*, 20, 1070–1083, 2012.

## Phytoplankton community structure in the North Sea

M. Thyssen et al.

Title Page

Abstract

Introduction

Conclusions

References

Tables

Figures



Back

Close

Full Screen / Esc

Printer-friendly Version

Interactive Discussion



## Phytoplankton community structure in the North Sea

M. Thyssen et al.

Title Page

Abstract

Introduction

Conclusions

References

Tables

Figures



Back

Close

Full Screen / Esc

Printer-friendly Version

Interactive Discussion



Alvain, S., Le Quéré, C., Bopp, L., Racault, M. F., Beaugrand, G., Dessailly, D., and Buitenhuis, E.: Rapid climatic driven shifts of diatoms at high latitudes, *Remote Sens. Environ.*, 132, 195–201, 2013.

Ben Mustapha, Z., Alvain, S., Jamet, C., Loisel, H., and Dessailly, D.: Automatic classification of water leaving radiance anomalies from global SeaWiFS imagery: application to the detection of phytoplankton groups in open ocean waters, *Remote Sens. Environ.*, RSE-08794, doi:10.1016/j.rse.2013.08.046, 2014.

Boyce, D. G., Lewis, M. R., and Worm, B.: Global phytoplankton decline over the past century, *Nature*, 466, 591–596, 2010.

Buma, A. G. J., W. W. C. Gieskes and Thomsen, H. A.: Abundance of cryptophyceae and chlorophyll b-containing organisms in the Weddell-Scotia Confluence area in the spring of 1988, *Polar Biol.*, 12, 43–52, 1992.

Burkill, P. H., Archer, S. D., Robinson, C., Nightingale, P. D., Groom, S. B., Tarran, G. A., and Zubkov, M. V.: Dimethyl sulphide biogeochemistry within a coccolithophore bloom (DISCO): an overview, *Deep-Sea Res. Pt. II*, 49, 2863–2885, 2002.

Chase, A., Boss, E., Zaneveld, R., Bricaud, A., Claustre, H., Ras, J., Dall'Olmo, G., and Westberry, T. K.: Decomposition of in situ particulate absorption spectra, *Meth. Oceanogr.*, 7, 110–124, 2013.

Chisholm, S. W., Olson, R. J., and Yentsch, C. M.: Flow cytometry in oceanography: status and prospects, *Eos T. Am. Geophys. Un.*, 69, 562–572, 1988.

Ciotti, A. and Bricaud, A.: Retrievals of a size parameter for phytoplankton and spectral light absorption by Colored Detrital Matter from water-leaving radiances at SeaWiFS channels in a continental shelf region off Brazil, *Limnol. Oceanogr.-Meth.*, 4, 237–253, 2006.

Claustre, H., Hooker, S. B., Van Heukelem, L., Berthon, J.-F., Barlow, R., Ras, J., Sessions, H., Targa, C., Thomas, C. S., van der Linde, D., and Marty, J.-C.: An intercomparison of HPLC phytoplankton pigment methods using in situ samples: application to remote sensing and database activities, *Mar. Chem.*, 85, 41–61, 2004.

Colin, P., I., Le Quéré, C., Buitenhuis, E., House, J., Klaas, C., and Knorr, W.: Biosphere Dynamics: Challenges for Earth System Models. *The State of the Planet: Frontiers and Challenges*, edited by: Hawkesworth, C. J. and Sparks, R. S. J., American Geophysical Union, 2004.

## Phytoplankton community structure in the North Sea

M. Thyssen et al.

[Title Page](#)

[Abstract](#)

[Introduction](#)

[Conclusions](#)

[References](#)

[Tables](#)

[Figures](#)



[Back](#)

[Close](#)

[Full Screen / Esc](#)

[Printer-friendly Version](#)

[Interactive Discussion](#)



- de Boyer Montégut, C., Madec, G., Fischer, A. S., Lazar, A., and Iudicone, D.: Mixed layer depth over the global ocean: an examination of profile data and a profile-based climatology, *J. Geophys. Res.-Oceans*, 109, C12003, doi:10.1029/2004JC002378, 2004.
- Demarcq, H., Reygondeau, G., Alvain, S., and Vantrepotte, V.: Monitoring marine phytoplankton seasonality from space, *Remote Sens. Environ.*, 117, 211–222, 2011.
- Dodge, J. D.: The early summer bloom of dinoflagellates in the North Sea, with special reference to 1971, *Mar. Biol.*, 40, 327–336, 1977.
- D'Ovidio, F., De Monte, S., Alvain, S., Dandonneau, Y., and Levy, M.: Fluides dynamical niches of phytoplankton types, *P. Natl. Acad. Sci. USA*, 107, 18366–18370, doi:10.1073/pnas.1004620107, 2010.
- Dubelaar, B. J., Gerritzen, P., Beeker, A. E. R., Jonker, R., and Tangen, K.: Design and first results of Cytobuoy: a wireless flow cytometer for in situ analysis of marine and fresh waters, *Cytometry*, 37, 247–254, 1999.
- Everitt, B. S. and Hothorn, T.: *A Handbook of Statistical Analyses Using R*, Chapman & Hall, 2006.
- Field, C. B., Behrenfeld, M. J., Randerson, J. T., and Falkowski, P. G.: Primary production of the biosphere: integrating terrestrial and oceanic components, *Science*, 281, 237–240, 1998.
- Foladori, P., Quaranta, A., and Ziglio, G.: Use of silica microspheres having refractive index similar to bacteria for conversion of flow cytometric forward light scatter into biovolume, *Water Res.*, 42, 3757–3766, 2008.
- Gailhard, I., Gros, P., Durbec, J. P., Beliaeff, B., Belin, C., Nézan, E., and Lassus, P.: Variability patterns of microphytoplankton communities along the French coasts, *Mar. Ecol.-Prog. Ser.*, 242, 39–50, 2002.
- Gomez, F. and Souissi, S.: Unusual diatoms linked to climatic events in the northeastern English Channel, *J. Sea Res.*, 58, 283–290, 2007.
- Guiselin, N.: *Etude de la Dynamique des Communautés Phytoplanktoniques par Microscopie et Cytométrie en Flux, en Eaux Côtieres de la Manche Orientale*, Ph.D. thesis, Biological Oceanology, University of Littoral Côte d'Opale (ULCO), ULCO-MREN, 190 pp., 2010.
- Hirata, T., Hardman-Mountford, N. J., Brewin, R. J. W., Aiken, J., Barlow, R., Suzuki, K., Isada, T., Howell, E., Hashioka, T., Noguchi-Aita, M., and Yamanaka, Y.: Synoptic relationships between surface Chlorophyll-*a* and diagnostic pigments specific to phytoplankton functional types, *Biogeosciences*, 8, 311–327, doi:10.5194/bg-8-311-2011, 2011.

## Phytoplankton community structure in the North Sea

M. Thyssen et al.

Title Page

Abstract

Introduction

Conclusions

References

Tables

Figures



Back

Close

Full Screen / Esc

Printer-friendly Version

Interactive Discussion



- Holligan, P. M., Aarup, T., and Groom, S. B.: The North Sea: satellite colour atlas, Cont. Shelf Res., 9, 667–765, 1989.
- Houghton, S. D.: Coccolith sedimentation and transport in the North Sea, Mar. Geol., 99, 267–274, 1991.
- 5 Kaufman, L. and Rousseeuw, P. J.: Finding Groups in Data: an Introduction to Cluster Analysis, Wiley-Interscience, 1990.
- Kostadinov, T. S., Siegel, D. A., and Maritorena, S.: Retrieval of the particle size distribution from satellite ocean color observations, J. Geophys. Res., 114, C09015, doi:10.1029/2009JC005303, 2009.
- 10 Kruskopf, M. and Flynn, K. J.: Chlorophyll content and fluorescence responses cannot be used to gauge phytoplankton biomass, nutrient status or growth rate, New Phytol., 169, 525–536, 2006.
- Le Quéré, C. L., Harrison, S. P., Prentice, I. C., Buitenhuis, E. T., Aumont, O., Bopp, L., Claustre, H., Cotrim Da Cunha, L., Geider, R., Giraud, X., Klaas, C., Kohfeld, K. E., Legendre, L., Manizza, M., Platt, T., Rivkin, R. B., Sathyendranath, S., Uitz, J., Watson, A. J., and Wolf-Gladrow, D.: Ecosystem dynamics based on plankton functional types for global ocean biogeochemistry models, Glob. Change Biol., 11, 2016–2040, 2005.
- 15 Leterme, S., Seuront, L., and Edwards, M.: Differential contribution of diatoms and dinoflagellates to phytoplankton biomass in the NE Atlantic Ocean and the North Sea, Mar. Ecol.-Prog. Ser., 312, 57–65, 2006.
- Leterme, S., Pingree, R. D., Skogen, M. D., Seuront, L., Reid, P. C., and Attrill, M. J.: Decadal fluctuations in North Atlantic water inflow in the North Sea between 1958–2003: impact on temperature and phytoplankton populations, Oceanologia, 50, 59–72, 2008.
- Li, W. K. W.: Primary production of prochlorophytes, cyanobacteria and eukaryotic ultraphytoplankton: measurements from flow cytometric sorting, Limnol. Oceanogr., 39, 169–175, 1994.
- 25 Lomas, M. W., Roberts, N., Lipschultz, F., Krause, J. W., Nelson, D. M., and Bates, N. R.: Biogeochemical responses to late-winter storms in the Sargasso Sea. IV. Rapid succession of major phytoplankton groups, Deep-Sea Res. Pt. I, 56, 892–909, 2009.
- 30 Lorenzen, C. J.: A method for the continuous measurement of in vivo chlorophyll concentration, Deep-Sea Res. Pt. I, 13, 223–227, 1966.

## Phytoplankton community structure in the North Sea

M. Thyssen et al.

Title Page

Abstract

Introduction

Conclusions

References

Tables

Figures



Back

Close

Full Screen / Esc

Printer-friendly Version

Interactive Discussion



- Marinov, I., Doney, S. C., and Lima, I. D.: Response of ocean phytoplankton community structure to climate change over the 21st century: partitioning the effects of nutrients, temperature and light, *Biogeosciences*, 7, 3941–3959, doi:10.5194/bg-7-3941-2010, 2010.
- Masotti, I., Moulin, C., Alvain, S., Bopp, L., Tagliabue, A., and Antoine, D.: Large-scale shifts in phytoplankton groups in the Equatorial Pacific during ENSO cycles, *Biogeosciences*, 8, 539–550, doi:10.5194/bg-8-539-2011, 2011.
- Mendes, C. R. B., Tavano, V. M., Leal, M. C., Souza, M. S., Brotas, V., and Garcia, C. A. E.: Shifts in the dominance between diatoms and cryptophytes during three late summers in the Bransfield Strait (Antarctic Peninsula), *Polar Biol.*, 36, 537–547, 2013.
- Moisan, T. A. H., Sathyendranath, S., and Bouman, H. A.: Ocean Color Remote Sensing of Phytoplankton Functional Types, InTech, 2012.
- Moline, M. A., Claustre, H., Frazer, T. K., Schofield, O., and Vernet, M.: Alteration of the food web along the Antarctic Peninsula in response to a regional warming trend, *Glob. Change Biol.*, 10, 1973–1980, 2004.
- Nair, A., Sathyendranath, S., Platt, T., Morales, J., Stuart, V. M.-H, Forget, N., Devred, E., and Bouman, H.: Remote sensing of phytoplankton functional types, *Remote Sens. Environ.*, 112, 3366–3375, 2008.
- Nielsen, T. G., Lokkegaard, B., Richardson, K., Pedersen, F., and Hansen, L.: Structure of plankton communities in the Dogger Bank area (North Sea) during a stratified situation, *Mar. Ecol.-Prog. Ser.*, 95, 115–131, 1993.
- Olson, R. J., Shalapyonok, A., and Sosik, H. M.: An automated flow cytometer for analyzing pico- and nanophytoplankton=FlowCytobot, *Deep-Sea Res. Pt. I*, 50, 301–315, 2003.
- Racault, M. F., Le Quéré, C., Buitenhuis, E., Sathyendranath, S., and Platt, T.: Phytoplankton phenology in the global ocean, *Ecol. Indic.*, 14, 152–163, 2013.
- Ribalet, F., Marchetti, A., Hubbard, K. A., Brown, K., Durkin, C. A., Morales, R., Robert, M., Swalwell, J. E., Tortell, P. D., and Armbrust, E. V.: Unveiling a phytoplankton hotspot at a narrow boundary between coastal and offshore waters, *P. Natl. Acad. Sci. USA*, 107, 16571–16576, 2010.
- Rousseau, V., Chrétiennot-Dinet, M.-J., Jacobsen, A., Verity, P., and Whipple, S.: The life cycle of Phaeocystis: state of knowledge and presumptive role in ecology, *Biogeochemistry*, 83, 29–47, 2007.
- Rutten, T. P. A., Sandee, B., and Hofman, A. R. T.: Phytoplankton monitoring by high performance flow cytometry: a successful approach?, *Cytom. Part A*, 64, 16–26, 2005.

## Phytoplankton community structure in the North Sea

M. Thyssen et al.

[Title Page](#)

[Abstract](#)

[Introduction](#)

[Conclusions](#)

[References](#)

[Tables](#)

[Figures](#)



[Back](#)

[Close](#)

[Full Screen / Esc](#)

[Printer-friendly Version](#)

[Interactive Discussion](#)



Sharples, J., Moore, C. M., Hickman, A. E., Holligan, P. M., Tweddle, J. F., Palmer, M. R., and Simpson, J. H.: Internal tidal mixing as a control on continental margin ecosystems, *Geophys. Res. Lett.*, 36, L23603, doi:10.1029/2009GL040683, 2009.

Sathyendranath, S., Louisa, W., Emmanuel, D., Trevor, P., Carla, C., and Heidi, M.: Discrimination of diatoms from other phytoplankton using ocean-colour data, *Mar. Ecol.-Prog. Ser.*, 272, 59–68, 2004.

Sosik, H. M., Olson, R. J., Neubert, M. G., and Shalapyonok, A.: Growth rates of coastal phytoplankton from time-series measurements with a submersible flow cytometer, *Limnol. Oceanogr.*, 48, 1756–1765, 2003.

Thyssen, M., Tarran, G. A., Zubkov, M. V., Holland, R. J., Gregori, G., Burkill, P. H., and Denis, M.: The emergence of automated high-frequency flow cytometry: revealing temporal and spatial phytoplankton variability, *J. Plankton Res.*, 30, 333–343, 2008a.

Thyssen, M., Mathieu, D., Garcia, N., and Denis, M.: Short-term variation of phytoplankton assemblages in Mediterranean coastal waters recorded with an automated submerged flow cytometer, *J. Plankton Res.*, 30, 1027–1040, 2008b.

Thyssen, M., Garcia, N., and Denis, M.: Sub meso scale phytoplankton distribution in the North East Atlantic surface waters determined with an automated flow cytometer, *Biogeosciences*, 6, 569–583, doi:10.5194/bg-6-569-2009, 2009.

Uitz, J., Claustre, H., Gentili, B., and Stramski, D.: Phytoplankton class-specific primary production in the world's oceans: seasonal and interannual variability from satellite observations, *Global Biogeochem. Cy.*, 24, GB3016, doi:10.1029/2009GB003680, 2010.

Van Bleijswijk, J. D. L., Kempers, R. S., Veldhuis, M. J., and Westbroek, P.: Cell and growth characteristics of types A and B of *Emiliania huxleyi* (Prymnesiophyceae) as determined by flow cytometry and chemical analyses, *J. Phycol.*, 30, 230–241, 1994.

Van Heukelem, L. and Thomas, C. S.: Computer assisted high performance liquid chromatography method development with applications to the isolation and analysis of phytoplankton pigments, *J. Chromatogr.*, 910, 31–49, 2001.

Vantrepotte, V., Loisel, H., Dessailly, D., and Mériaux, X.: Optical classification of contrasted coastal waters, *Remote Sens. Environ.*, 123, 306–323, 2012.

Vargas, M., Brown, C. W., and Sapiano, M. R. P.: Phenology of marine phytoplankton from satellite ocean color measurements, *Geophys. Res. Lett.*, 36, L01608, doi:10.1029/2008GL036006, 2009.

- Veldhuis, M. J. W. and Kraay, G. W.: Application of flow cytometry in marine phytoplankton research: current applications and future perspectives, *Sci. Mar.*, 64, 121–134, 2000.
- Waterbury, J. B., Watson, S. W., Guillard, R. R. L., and Brand, L. E.: Widespread occurrence of a unicellular, marine, planktonic cyanobacterium, *Nature*, 277, 293–294, doi:10.1038/277293a0, 1979.
- 5 Werdell, P. J., Proctor, C. W., Boss, E., Leeuw, T., and Ouhssain, M.: Underway sampling of marine inherent optical properties on the Tara Oceans expedition as a novel resource for ocean color satellite data product validation, *Meth. Oceanogr.*, 7, 40–51, 2013.
- Widdicombe, C. E., Eloire, D., Harbour, D., Harris, R. P., and Somerfield, P. J.: Long-term phytoplankton community dynamics in the Western English Channel, *J. Plankton Res.*, 32, 643–655, 2010.
- 10 Wiltshire, K. H. and Manly, B. F. J.: The warming trend at Helgoland Roads, North Sea: phytoplankton response, *Helgoland Mar. Res.*, 58, 269–273, 2004.
- Zubkov, M. V. and Burkill, P. H.: Syringe pumped high speed flow cytometry of oceanic phytoplankton, *Cytom. Part A*, 69, 1010–1019, 2006.
- 15 Zubkov, M. V. and Quartly, G. D.: Ultraplankton distribution in surface waters of the Mozambique Channel – flow cytometry and satellite imagery, *Aquat. Microb. Ecol.*, 33, 155–161, 2003.

---

## Phytoplankton community structure in the North Sea

M. Thyssen et al.

---

[Title Page](#)[Abstract](#)[Introduction](#)[Conclusions](#)[References](#)[Tables](#)[Figures](#)[Back](#)[Close](#)[Full Screen / Esc](#)[Printer-friendly Version](#)[Interactive Discussion](#)

## Phytoplankton community structure in the North Sea

M. Thyssen et al.

[Title Page](#)

[Abstract](#)

[Introduction](#)

[Conclusions](#)

[References](#)

[Tables](#)

[Figures](#)



[Back](#)

[Close](#)

[Full Screen / Esc](#)

[Printer-friendly Version](#)

[Interactive Discussion](#)



**Table 1.** Minimal, maximal, average and SD of abundance ( $\text{cells cm}^{-3}$ ) for each defined phytoplankton cluster followed by the size estimated ( $\mu\text{m}$ ) average  $\pm$  SD values.

Cluster's name	Abundance min–max ( $\text{cells cm}^{-3}$ )	Average abundance $\pm$ SD ( $\text{cells cm}^{-3}$ )	Average size $\pm$ SD ( $\mu\text{m}$ )
PicoORG	25–18 710	1559 $\pm$ 2821	1.09 $\pm$ 0.17
PicoRED	275–26 960	5674 $\pm$ 4647	1.83 $\pm$ 0.32
NanoRED1	97–7172	888 $\pm$ 942	2.33 $\pm$ 0.33
NanoORG	< 10–759	87 $\pm$ 150	5.8 $\pm$ 2.1
NanoSWS	< 10–376	99 $\pm$ 93	10 $\pm$ 2.56
NanoRED2	200–54 880	4187 $\pm$ 7878	6.4 $\pm$ 1.4
Micro1	< 10–4392	420 $\pm$ 769	16.9 $\pm$ 5.6
MicroORG	< 10–306	48 $\pm$ 60	23.5 $\pm$ 10
MicroLowORG	< 10–687	69 $\pm$ 111	23.75 $\pm$ 8.6
Micro2	< 10–420	37 $\pm$ 59	65.5 $\pm$ 21.0

## Phytoplankton community structure in the North Sea

M. Thyssen et al.

[Title Page](#)

[Abstract](#)

[Introduction](#)

[Conclusions](#)

[References](#)

[Tables](#)

[Figures](#)

[◀](#)

[▶](#)

[◀](#)

[▶](#)

[Back](#)

[Close](#)

[Full Screen / Esc](#)

[Printer-friendly Version](#)

[Interactive Discussion](#)



**Table 2.** Spearman's rank correlation coefficient between the different methods used for chlorophyll *a* estimates and with the Total TFLR from the scanning flow cytometer per unit volume.

Spearman's correlation coefficient	SFC TFLR cm <sup>-3</sup> (a.u.) <i>n</i> = 247	AOA fluorometer (μg dm <sup>-3</sup> ) <i>n</i> = 254	HPLC chl <i>a</i> (μg dm <sup>-3</sup> ) <i>n</i> = 12	Turner chl <i>a</i> (μg dm <sup>-3</sup> ) <i>n</i> = 9
SFC TFLR cm <sup>-3</sup> (a.u.)	1	0.93*	0.82*	0.82*
AOA fluorometer (μg dm <sup>-3</sup> )		1	0.86*	0.82*
HPLC chl <i>a</i> (μg dm <sup>-3</sup> )			1	0.98*
Turner chl <i>a</i> (μg dm <sup>-3</sup> )				1

\*  $p < 0.001$ .

## BGD

11, 15621–15662, 2014

Phytoplankton  
community structure  
in the North Sea

M. Thyssen et al.

[Title Page](#)[Abstract](#)[Introduction](#)[Conclusions](#)[References](#)[Tables](#)[Figures](#)[Back](#)[Close](#)[Full Screen / Esc](#)[Printer-friendly Version](#)[Interactive Discussion](#)**Table 3.** Minimal and maximal anomaly (Ra) values for each collected MODIS wavelength (nm) that characterizes the edges for the two PHYSAT radiance anomalies spectra (N1 and N2) observed in this study.

Node	Ra (412) nm		Ra (443) nm		Ra (488) nm		Ra (531) nm	
	Min	Max	Min	Max	Min	Max	Min	Max
N1 ( $n = 5$ )	1.06	1.30	0.96	1.24	0.91	1.10	0.91	1.09
N2 ( $n = 10$ )	0.74	0.97	0.75	0.93	0.70	0.89	0.72	0.93

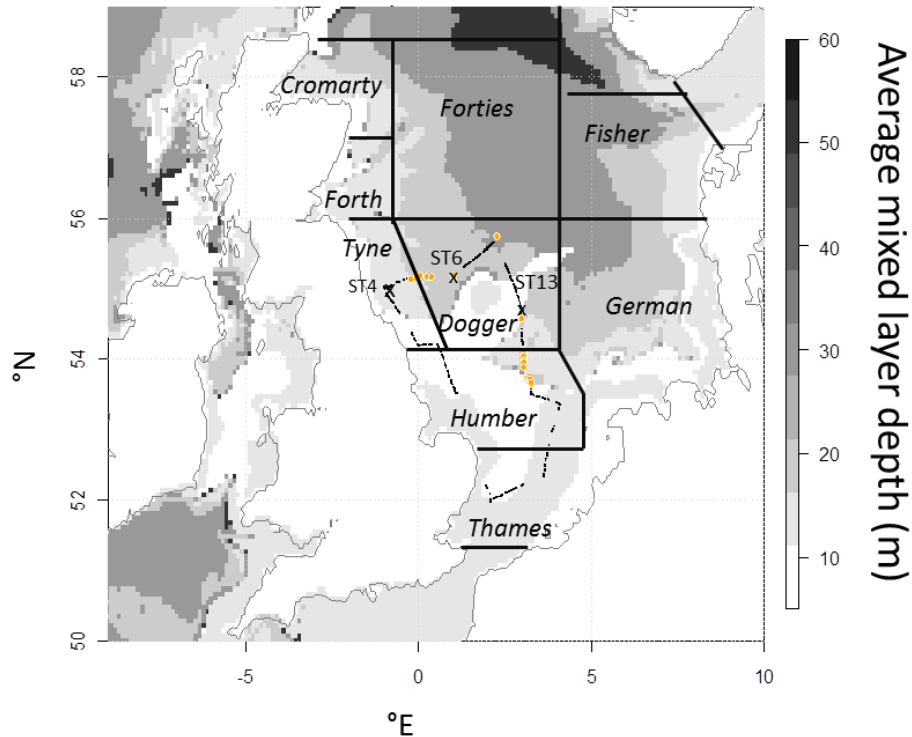


**Figure 1.** Flow cytometry sampling points superimposed on the mixed layer depth (m) calculated with modeled temperature of the water column from the FOAM AMM7 (average values from the 8 to the 12 May 2011). Chosen stations for phytoplankton pictures collection with the flow cytometer are labeled (ST = station, ST4, ST6, ST13). Yellow squares correspond to MODIS matching points for non-turbid waters selected between 06:00 and 18:00 UTC

## BGD

11, 15621–15662, 2014

### Phytoplankton community structure in the North Sea

M. Thyssen et al.

Title Page

Abstract

Introduction

Conclusions

References

Tables

Figures



Back

Close

Full Screen / Esc

Printer-friendly Version

Interactive Discussion



---

**Phytoplankton  
community structure  
in the North Sea**

M. Thyssen et al.

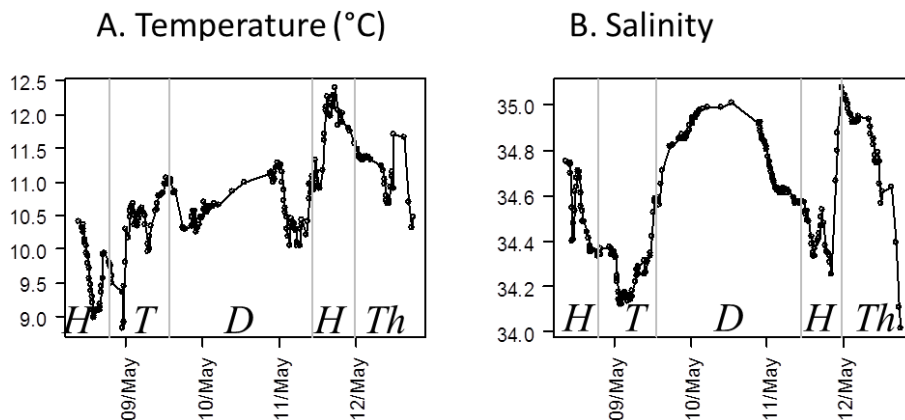


**Figure 2.** (a) Temperature and (b) salinity measured with the Pocket Ferry Box. Presented data is selected to match the scanning flow cytometry collected samples. Grey bars delimit the traversed marine areas: H = Humber, T = Tyne, D = Dogger, Th = Thames.

[Title Page](#)[Abstract](#)[Introduction](#)[Conclusions](#)[References](#)[Tables](#)[Figures](#)[Back](#)[Close](#)[Full Screen / Esc](#)[Printer-friendly Version](#)[Interactive Discussion](#)

Phytoplankton  
community structure  
in the North Sea

M. Thyssen et al.

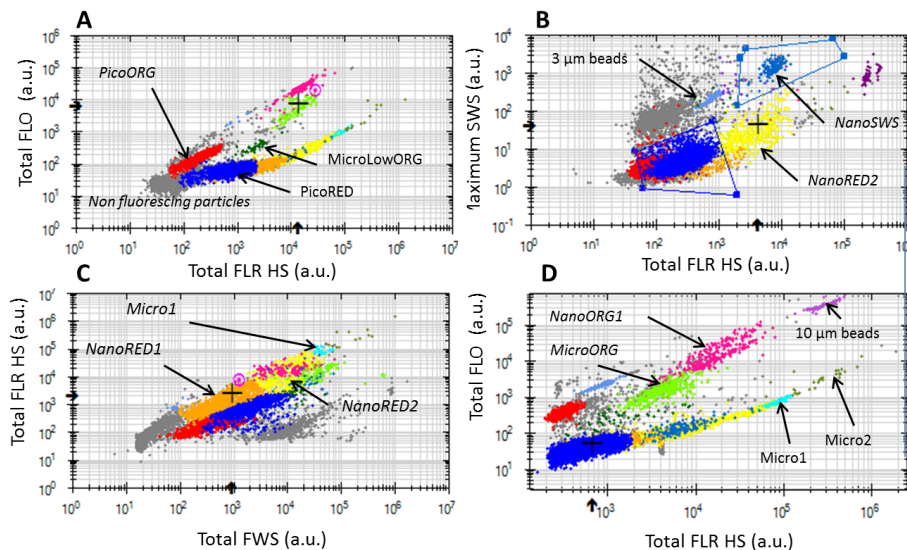


**Figure 3.** (a) TFLO vs. TFLR (a.u.) cytogram with a trigger level at 10 mV showing the PicoORG cluster, the PicoRED cluster, the MicroLowORG cluster. (b) Maximum SWS (a.u.) vs. TFLR (a.u.) cytogram with a trigger level at 10 mV showing the NanoSWS cluster, the NanoRED2 cluster and 3  $\mu\text{m}$  beads. (c) TFLR (a.u.) vs. TFWS (a.u.) cytogram with a trigger level at 10 mV showing the NanoRED1 cluster, the NanoRED2 cluster, and the Micro1 cluster. (d) TFLO vs. TFLR (a.u.) cytogram with a trigger level of 25 mV showing the NanoORG1, the MicroORG, the Micro1 and Micro2 clusters and 10  $\mu\text{m}$  beads.

Title Page	
Abstract	Introduction
Conclusions	References
Tables	Figures
◀	▶
◀	▶
Back	Close
Full Screen / Esc	
Printer-friendly Version	
Interactive Discussion	





Phytoplankton  
community structure  
in the North Sea

M. Thyssen et al.

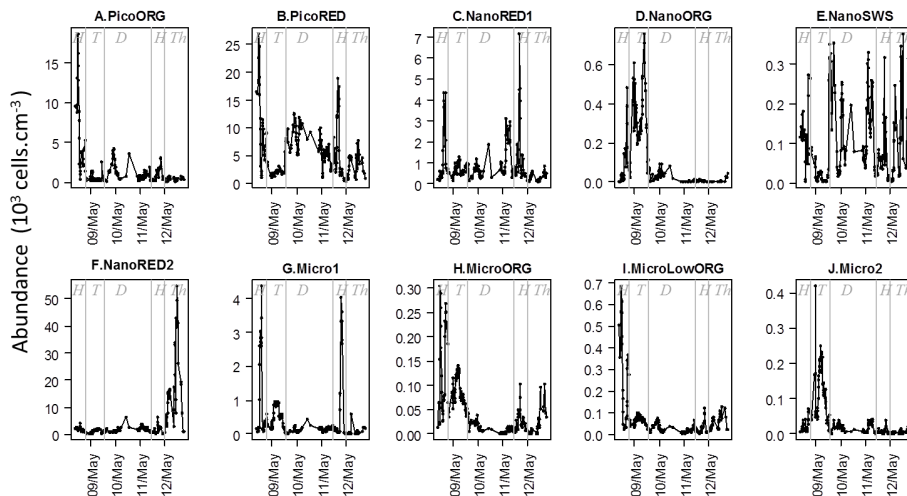


**Figure 5.** Abundance ( $10^3 \text{ cells cm}^{-3}$ ) of each phytoplankton cluster resolved with the scanning flow cytometer. Scales are not homogenised for the purpose of distribution evidence. Grey bars separate the traversed marine areas: H = Humber, T = Tyne, D = Dogger, Th = Thames.

Title Page

Abstract

Introduction

Conclusions

References

Tables

Figures



Back

Close

Full Screen / Esc

Printer-friendly Version

Interactive Discussion



Phytoplankton  
community structure  
in the North Sea

M. Thyssen et al.

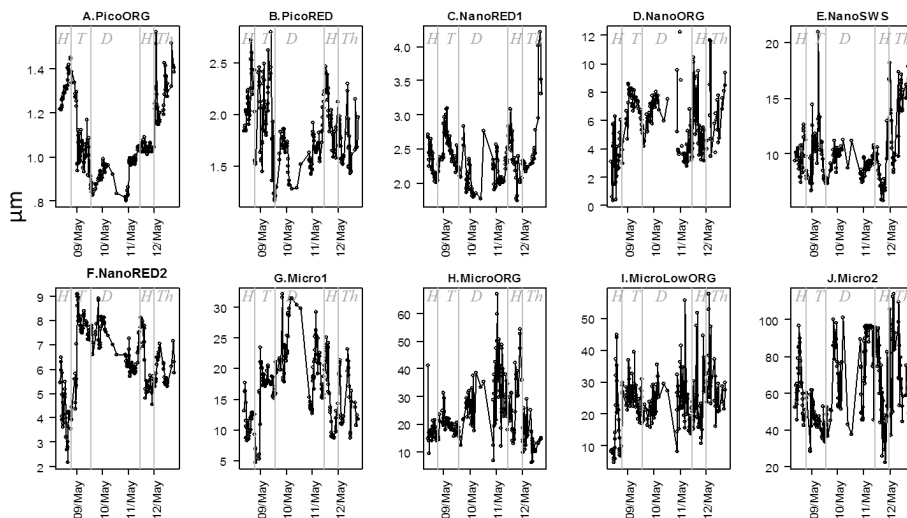


**Figure 6.** Average estimated size for each phytoplankton cluster resolved with the scanning flow cytometer. Scales are not homogenised for the purpose of distribution evidence. Grey bars separate the traversed marine areas: H = Humber, T = Tyne, D = Dogger, Th = Thames.

Title Page

Abstract

Introduction

Conclusions

References

Tables

Figures



Back

Close

Full Screen / Esc

Printer-friendly Version

Interactive Discussion



Phytoplankton  
community structure  
in the North Sea

M. Thyssen et al.

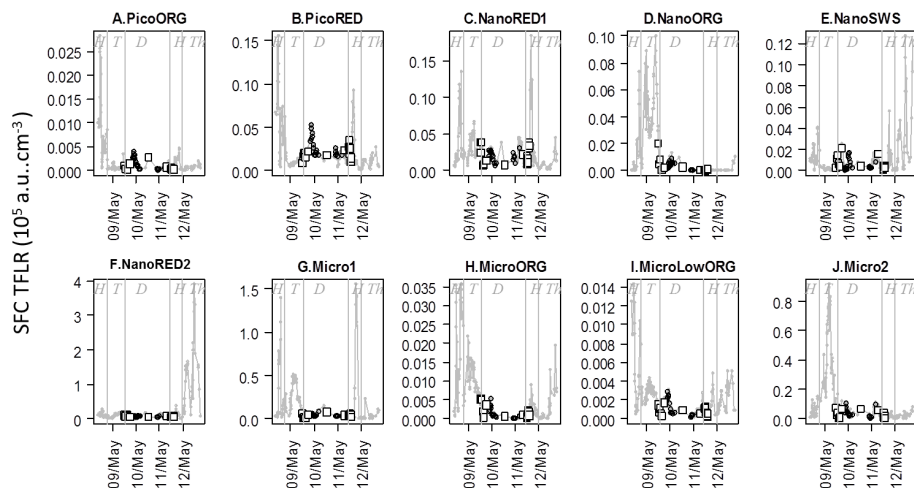


**Figure 7.** Scanning flow cytometer Total red fluorescence per unit volume (SFC TFLR  $\text{cm}^{-3}$ ) for each phytoplankton cluster. Superimposed large black squares are the matching points with MODIS pixels in non-turbid waters between 06:00 and 18:00 UTC. Small black squares correspond to the night SFC samples matching MODIS passage but not taken into account because of the possible differences between day and night community structures. Scales are not homogenised for the purpose of distribution evidence. Grey bars separate the traversed marine areas: H = Humber, T = Tyne, D = Dogger, Th = Thames.

Title Page

Abstract

Introduction

Conclusions

References

Tables

Figures



Back

Close

Full Screen / Esc

Printer-friendly Version

Interactive Discussion



## Phytoplankton community structure in the North Sea

M. Thyssen et al.

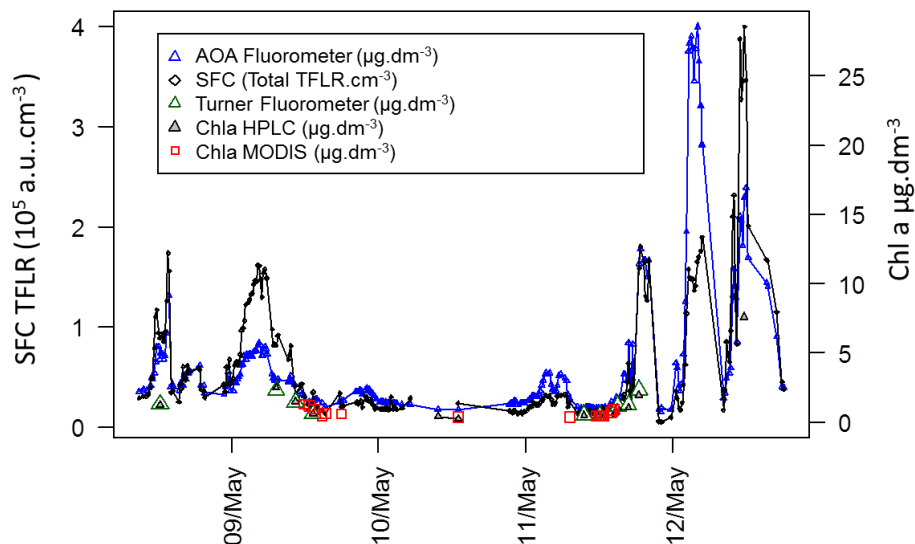


**Figure 8.** SFC Total TFLR per  $\text{cm}^{-3}$  compared to chl *a* analyses using different instruments. Refer to Material and Methods for a detailed description of each method. Blue triangles: AOA fluorometer PFB (chl *a*  $\mu\text{g}\cdot\text{dm}^{-3}$ ). Black diamonds: SFC Total TFLR  $\text{cm}^{-3}$  ( $\text{a.u.}\cdot\text{cm}^{-3}$ ). Green triangles: Turner fluorometer (chl *a*  $\mu\text{g}\cdot\text{dm}^{-3}$ ). Grey triangles: HPLC (chl *a*  $\mu\text{g}\cdot\text{dm}^{-3}$ ). Red squares: MODIS chl *a* values corresponding to non-turbid waters (after Vantrepotte et al., 2012) and selected between 06:00 and 18:00 UTC (chl *a*  $\mu\text{g}\cdot\text{dm}^{-3}$ ).

Title Page

Abstract

Introduction

Conclusions

References

Tables

Figures



Back

Close

Full Screen / Esc

Printer-friendly Version

Interactive Discussion



Phytoplankton  
community structure  
in the North Sea

M. Thyssen et al.

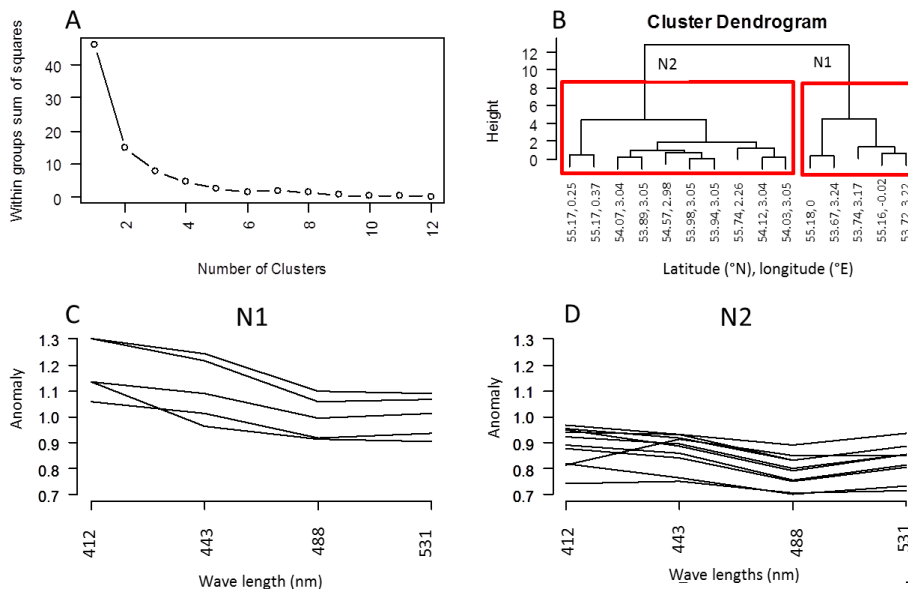


**Figure 9.** (a) Within sum of squares for the optimal number of K-nodes selection corresponding to PHYSAT anomalies. (b) Cluster dendrogram defining the two main nodes grouping similar PHYSAT anomalies matchups (N1 and N2). (c and d) corresponding nLw\* spectra for N1 and N2.

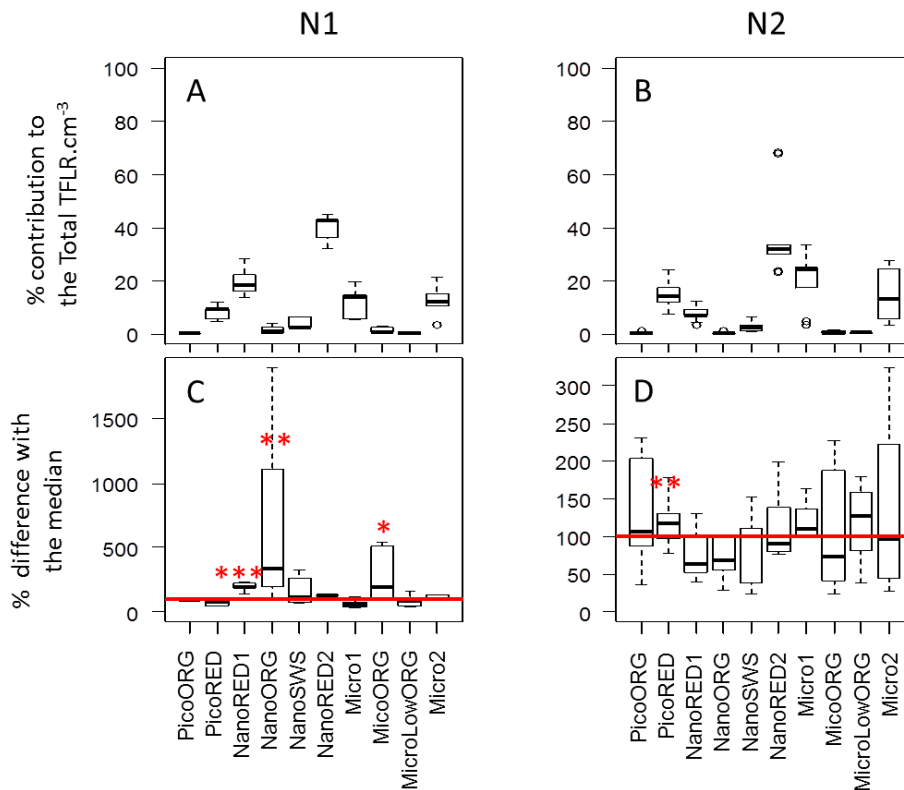


**Figure 10.** (a and b) Clusters proportional contribution to the Total TFLR $\text{cm}^{-3}$  within each PHYSAT anomaly (N1 and N2). (c and d) Within each anomaly, clusters TFLR $\text{cm}^{-3}$  proportional difference to its median value calculated on the entire matching points dataset. Wilcoxon rank test was run for each cluster between the two anomalies. \*\*\*  $p < 0.001$ , \*\*  $p < 0.01$ , \*  $p < 0.1$ .

[Title Page](#)
[Abstract](#)
[Introduction](#)
[Conclusions](#)
[References](#)
[Tables](#)
[Figures](#)

[Back](#)
[Close](#)
[Full Screen / Esc](#)
[Printer-friendly Version](#)
[Interactive Discussion](#)


## Phytoplankton community structure in the North Sea

M. Thyssen et al.

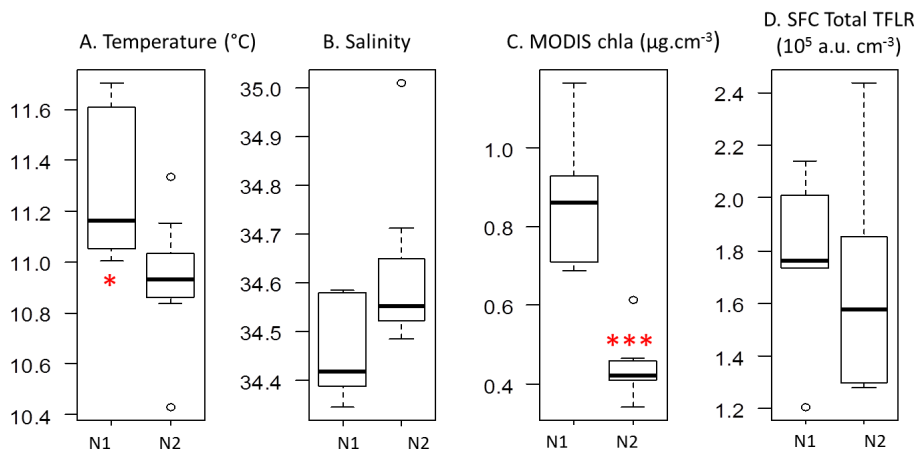


**Figure 11.** Boxplots within each PHYSAT anomaly (N1, N2) of **(a)** temperature ( $^{\circ}\text{C}$ ), **(b)** salinity, **(c)** chlorophyll *a* (as estimated from MODIS L3 Binned) and **(d)**, total TFLR ( $\text{a.u. cm}^{-3}$ ). Wilcoxon rank test was run for each parameter between the two anomalies. \*\*\*  $p < 0.001$ , \*\*  $p < 0.01$ , \*  $p < 0.1$ .

Title Page

Abstract

Introduction

Conclusions

References

Tables

Figures



Back

Close

Full Screen / Esc

Printer-friendly Version

Interactive Discussion



Phytoplankton  
community structure  
in the North Sea

M. Thyssen et al.

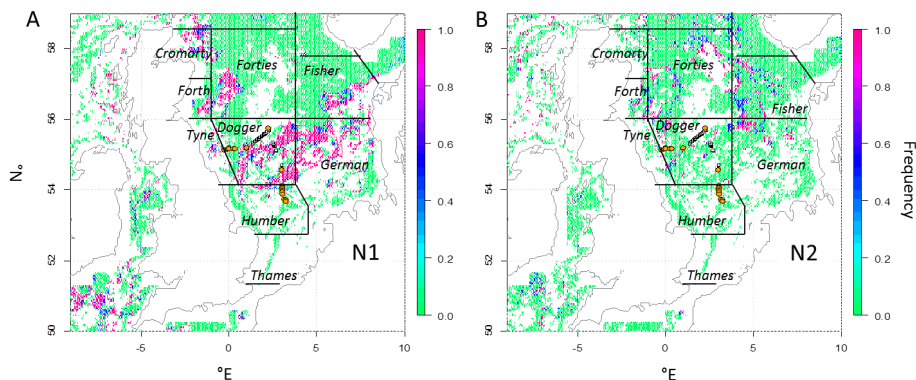


**Figure 12.** (a and b) Frequency of occurrence of the two distinct anomalies (N1 and N2) over the North Sea during the sampling period (8–12 May 2011).

[Title Page](#)[Abstract](#)[Introduction](#)[Conclusions](#)[References](#)[Tables](#)[Figures](#)[Back](#)[Close](#)[Full Screen / Esc](#)[Printer-friendly Version](#)[Interactive Discussion](#)